IGNITION PROCESSES OF PALM OIL BIODIESEL AND DIESEL FUELS USING A TWO STAGE LAGRANGIAN APPROACH

A. Alfazazi[*, 1], O. A. Kuti[2], S. M. Sarathy[1]

[1]King Abdullah University of Science and Technology, Thuwal, Jeddah, Saudi Arabia
[2]City University, London, United Kingdom

Abstract

The ignition characteristics of palm oil biodiesel and conventional diesel fuels are simulated using the two stage Lagrangian (TSL) 0-D modeling technique. For the diesel fuel surrogate, thermochemical and reaction kinetic data of n-heptane detailed mechanism was utilized. For the palm biodiesel, simulations were done using the reduced mechanisms for the palm oil biodiesel using mixture of methyl decanoate, methyl decenoate and n-heptane as surrogates. Validations of the simulated data were performed against experimental results. The simulation results were able to reproduce the experimental trends in the ignition delay. The chemical kinetic processes responsible for controlling ignition were investigated using the TSL model.

Introduction

Biodiesel is one of the promising alternative fuel sources. This is partly due to its capacity of reducing CO, soot and unburned hydrocarbon (UHC) emission. Many countries of Europe and USA are advocating for the use of alternative fuels. Recently, the top CO2 emitters; China and USA agreed to cut greenhouse gas (GHG) emissions by 28% and 20%, respectively, by the year 2030. Many advantages of using biodiesel as an alternative fuel can be found in [1-10]. Zhu et al. [1] and Deepak et al. [11] have reported that modern diesel engines can operate using biodiesel with significant reduction in emission and without a major change to their design. Biodiesels have only a limited number of major fatty acid methyl ester (FAME) components compared to the conventional diesel fuels. This made it possible to include all its components in experimental or kinetic model analysis [4]. The five major components of biodiesel include the unsaturated methyl oleate ($C_{19}H_{36}O_2$), methyl linoleate ($C_{19}H_{34}O_2$ and methyl linolenate ($C_{19}H_{32}O_2$) and the saturated methyl palmitate ($C_{17}H_{34}O_2$) and methyl stearate ($C_{19}H_{38}O_2$). According to Westbrook [4], most biodiesels that are produced from these five FAME components have similar (physical and chemical) properties to those of petroleum based fuels.

The diesel engine leads other power generating engines in the transportation sector both in terms of reliability and efficiency [12]. Notwithstanding, more studies are required in order to improve their efficiency. Temporal control of combustion events in an engine is an essential parameter affecting efficiency and exhaust gas emissions [12, 13]. One way to do this is by controlling the timing of ignition. Fuel ignition in diesel engines is achieved by compression of the stratified fuel/air charge. Therefore, timing of this event could be influenced by a variety of factors such as ambient temperature, ambient pressure, injection pressure and also by varying the concentration of O_2 in the cylinder. Several efforts were made by [12, 13, 14] to study ignition processes in diesel engines. They found that an increase in both injection pressure and ambient temperature decreases the ignition delay time (i.e. the time period between the start of injection to the onset of ignition).

Since there is a growing interest in the use of biodiesel and diesels fuels in the diesel engines, it becomes imperative to study the ignition processes of these fuels. As such, this work aims at unveiling the underlying phenomena affecting both diesel and biodiesel fuel ignition, together with comparing the ignition behavior of the two fuels using the two stage Lagrangian model. Simulations were validated using a previous experiment conducted using a constant volume combustion chamber by Kuti et al. [3].

Research methodology:

The two-stage lagrangian model

The two-stage Lagrangian (TSL) modeling technique was used to execute a zero dimensional (0-D) simulation of diesel surrogate and biodiesel surrogate spray combustion processes in the constant volume combustion chamber. The TSL model is a FORTRAN computer code that calculates the species mass fractions, reaction rates and temperature in a steady, non-premixed turbulent jet [12, 15]. The TSL model, unlike other 0-D models, was introduced to retain the ability to use detail chemical kinetics while also simulating basic mixing process that are important in turbulent gas-jet diffusion flames [16]. Unlike multidimensional CFD modeling techniques that rely on reduced mechanisms with less number of reactions and species, the TSL has the capability of using a large detailed reaction mechanism with little computational expense. Figure 1 gives a brief description of the model.

[*] Corresponding author: Adamu.Fazazi@kaust.edu.sa

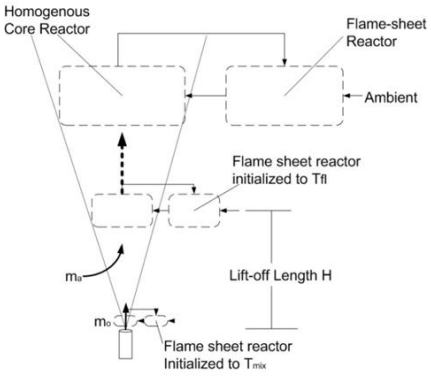

Figure 1. Schematic diagram of TSL model for turbulent Jets [17]

The model is from an experimental observation that reactions in gas jets occur in two layers: first starting in the diffusion layers and later proceeding to regions that are almost homogeneous as a result of turbulent mixing. Firstly, entrained hot ambient air from the surroundings mixes with the jet fluid in a stoichiometric proportion at the flame sheet region of the diffusion layer, and later, the products from the flame sheet reactor moves to the homogeneous reactor where they mixes homogenously with the fuel jet. This process will be continued up to the flame tip where the whole fuel is expended [12, 15, 16, 17].

The homogeneous layers are represented by a perfectly stirred reactor, while the diffusion can be modeled as either a one-dimensional strained diffusion flame or a perfectly stirred reactor. In this study, both the homogeneous region and the flame sheet were modeled as perfectly stirred reactors; this is because using the two-reactor model yields essentially the same results with the reactor-flame version, albeit at reduced computational cost [15].

The equations for the conservation of mass and energy which describes the flow field for the homogeneous reactors are as follows [15]:

$$\frac{dm_h}{dx} = f(x)$$

$$\frac{dY_{k,h}}{dx} = \frac{(1+B)}{m_h}\frac{dm_h}{dx}\left(Y_{k,f} - Y_{k,h}\right) + \left(\frac{\dot{\omega}_k W_k}{\rho}\right)_h \frac{1}{u} \quad k = 1,\ldots,K$$

$$\frac{dT_h}{dx} = \frac{(1+B)}{m_h c_p}\frac{dm_h}{dx}\sum_k Y_{k,f}\left(h_{k,f} - h_{k,h}\right) - \frac{1}{\rho_h u c_p} + \sum_k \left(h_k \dot{\omega}_k W_k\right)_h - \frac{\dot{q}_R}{u c_p}$$

$$B = \frac{\left(f_{st} - f_\infty\right)}{\left(\left|f_h - f_{st}\right| + \varepsilon\right)}$$

$$f = \sum_{k=1}^{K} \frac{Y_k}{W_k} \sum_{j=C,H} a_{j,k} M_j$$

And the conservation equations for the flame sheet reactors are:

$$0 = \frac{1}{\tau}\left[\left(Y_{k,\infty} - Y_{k,f}\right) + B\left(Y_{k,h} - Y_{k,f}\right)\right] + \left(\frac{\dot{\omega}_k W_k}{\rho}\right)_f \quad k = 1,\ldots,K$$

$$0 = \frac{1}{\tau c_p}\left[\sum_k Y_{k,\infty}\left(h_{k,\infty} - h_{k,f}\right) + B\sum_k Y_{k,h}\left(h_{k,h} - h_{k,f}\right)\right] - \frac{1}{\rho_f c_p}\sum_k \left(h_k \dot{\omega}_k W_k\right)_f - \frac{\dot{q}_R}{c_p}$$

Where x is the axial distance from the nozzle; $m=\rho uA$ is the axial mass flow rate; u is the average velocity in the axial direction; A is the jet cross-sectional area; Y_k is mass fraction of species k; K is the total number of species; T is the temperature; h_k is the enthalpy of species k; $\dot{\omega}_k$ is the molar production rate of species k; $_{Wk}$ is the molecular weight of species k; ρ is density; c_p is specific heat (at constant pressure); qR is the radiation loss; and subscripts h and f refer to the homogeneous and flame-sheet reactors. Where f is the fuel mixture fraction: mass of fuel elements per mass of mixture; $a_{j,I}$ is the number of atoms of element j in species k; M_j is the atomic mass of element j; the subscripts and st refer to the surroundings and the stoichiometric condition; and ε is a small number to avoid the singularity where f_h passes through stoichiometric.

The advantage of using the TSL model, apart from its ability to use detailed kinetic mechanism in a less computational time, is the fact that preparation of the code and its input is relatively easier than computational fluid dynamic (CFD) codes. Details of the formulation and description of TSL could be found in previous works [15, 16, 17, 18].

Approach

Two conditions can be studied using this model. The condition in which the diffusion flame reactor is turned off and secondly, a condition in which the lift-off is prescribed by a certain height. In this study, the diffusion flame reactor was turned off, by maintaining the temperature at flame sheet reactor at 350K. The homogeneous reactor ignites itself, allowing the analyses of mixing effects on ignition delay.

In running the TSL code, a detailed n-heptane reaction mechanism from LLNL with 1340 species and 5723 reactions [19] was utilized as the diesel surrogate. The reason for using n-heptane as a surrogate is because it has a cetane number of 56 comparable to that of a conventional diesel fuel [20]. As reported by Musculus et al. [21], n-heptane has similar ignition and apparent heat release rate (AHRR) behavior in engines to that of a typical diesel fuel. For palm biodiesel, simulations were performed using the reduced mechanisms (115 species and 460 reactions) for the palm oil biodiesel comprising a mixture of methyl decanoate, methyl decenoate and n-heptane as surrogates [2]. Details of their mixture composition could be found in [3, 5]. As stated earlier, validations of the simulated data for both diesel and the palm oil biodiesel were performed against previous experimental results using a constant volume combustion chamber, as reported in [3]. The experimental conditions used as a baseline condition for the simulation are presented in Table 1.

Table 1. Experimental conditions adopted for TSL simulation

Diesel Mechanism Reduced Biodiesel Mechanism	nC_7H_{16} LLNL[3] $C_{11}H_{20}O_2$(MD), $C_{11}H_{19}O_2$(MD9D), $C_{11}H_{19}O_2$(MD9D), nC_7H_{16}[2]
Ambient gas Pressure(MPa) Temperature(K)	Air 4.0 885
Nozzle diameter (mm) Injection duration (ms) Injection Pressure(MPa)	0.16 1.5 100, 200 and 300

The TSL code is only capable of handling gas phase simulation, so the liquid fuel sources in this study have to be initialized to a gas phase simulation [16]. Thus, the fuel temperature was reduced to 300K to give the same adiabatic flame temperature as the liquid fuel. Again, in order for the gas to have the same momentum and mass flow as the liquid fuel, the density of the liquid fuel was reduced and the orifice diameter was enlarged. Details on how to do this could be found in [16].

The mixing rate into the reactors is determined by empirical correlation for jet mixing as proposed by [17]:

$m/m_o=C\ (x/d_o)\ \sqrt{}\ (\rho_a/\rho_o)$

Where: m is mass flow in the jet; m_o is the initial jet mass flow; ρ_o jet source density. C is a constant (C is 0.32 for non-reacting jets. For reacting jets, heat release inhibits the rate of air entrainment, thereby reducing C to 0.16 for momentum driven flames). C is 0.16 is used for these simulations. For more details on the simulation method, please refer to [16].

Ignition delay

In diesel engines, ignition delay is the time difference between the start of injection (SOI) to the start of combustion (SOC) [12]. The ignition processes of fuels always results to an increase in chemical reaction rates and eventually leads to fuel branching. At higher temperatures, the main branching reactions usually involve H radicals reacting with molecular oxygen to form OH and O, while at lower temperatures, the system reactivity is governed by the decomposition of peroxy radicals into two OH radicals. The transition from low temperature to high temperature reactivity is typically driven by the formation of H_2O_2 and its subsequent decomposition to two OH radicals.

For fuels exhibiting two stage ignition behaviors, after the liquid fuel is injected, it vaporizes and mixes with hot air. When the mixture is fully vaporized, momentum conveys the fuel air mixture downstream of the liquid length, where it entrains hotter cylinder gases, and then first stage ignition is witnessed. This first stage heat release increases the temperature resulting in a net decrease of system reactivity due to negative temperature coefficient (NTC) reactions. After a while, the reactions progress into a more exothermic second stage ignition [21]. Thus, the ignition of typical diesel fuels is dominated by three distinct regimes: first stage ignition, NTC regime, and second stage ignition. It is therefore important to investigate the processes that influence these regimes of ignition. In this study, the second stage ignition delay time is taken as the time from the start of simulation to the time when the rate of change of temperature with time is maximum ((dT/dt)max).

Results and discussion

This study consists of four parts. First, the model is validated against experimental data, next, mass fraction analysis and rate of production analysis of some selected species at these two stages is presented. Finally, the second stage ignition regime is investigated in more detail.

Validation of ignition delay time:

The model was first validated against experiments performed at three different injection pressures, 100, 200 and 300MPa respectively, Fig. 2.

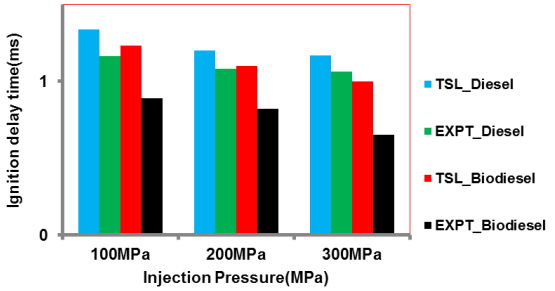

Figure 2. Validation of ignition delay time for diesel and biodiesel fuel at three different injection Pressures

For both diesel and biodiesel surrogates, there is a good agreement with the experiment especially in the ignition delay times. The trends was also well predicted showing that the ignition delay times decrease with increase injection pressure and those of biodiesel are shorter than diesel. Reasons for these trends are discussed in the next section. The quantitative agreement is also acceptable for both fuels. Simulated ignition delay times of biodiesel with reduced and detailed mechanisms are within 26 % and 76% of experimental values, and simulated diesel values for diesel fuel are within 12 % of experiments. The simulations over predict ignition delay times under all conditions.

Mass fraction and rate of production analysis:

In order to gain details into the chemical kinetics of the two-stage ignition behavior of diesel fuel surrogate, mass fraction, and rate of production analysis of some selected species of the diesel fuel surrogate as presented in Figs. 3 and 4. Species selection was based on reactions that have the highest rates of production at the first and second stage ignition delay time.

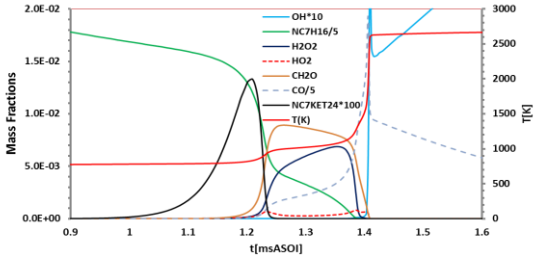

Figure 4a Mass fraction analysis at first stage ignition

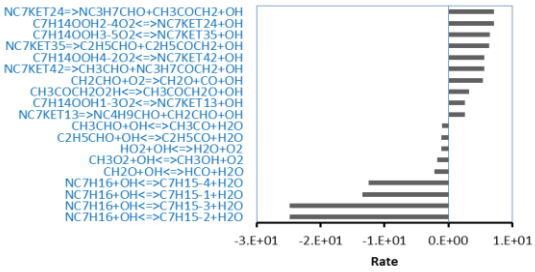

Figure 4a ROP analysis at first stage ignition

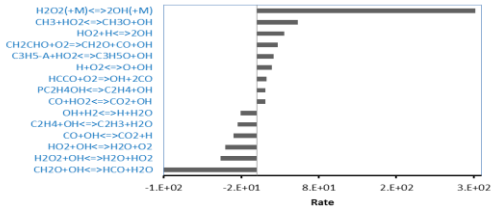

Figure 4b ROP analysis at first stage ignition

The temperature profile in Fig. 3 shows a well-defined two-stage ignition. In Fig 3, the first rise occurs at around 1.2ms. Here the temperature rises steadily until a stable temperature is achieved. The reactivity at this temperature is suppressed due to NTC reactions. After a brief period, at around 1.4ms, the temperature rises again very sharply and causing the second stage ignition.

The first rise (Fig. 3) is as a result of complicated kinetics of low temperature hydrocarbon combustion and this has relevance in practical combustion systems [23]. After H abstraction from the fuel by OH mainly, the fuel radical reacts with molecular O_2 to produce a peroxy radical. The fate of this radical depends on temperature. At high temperature, this radical fall apart and dissociate back to R and O_2. At low temperatures, the equilibrium is in favor of RO_2 (alkylperoxy radical). RO_2 isomerizes to QOOH (hydroperoxyalkyl radical), which later reacts with another O_2 molecule to O_2QOOH. This new molecule isomerizes and decomposes to ketohydroperoxide (KHP) plus two OH radical. Based on the reaction mechanism, the type of KHP species formed varies. In this study, NC7KET24 has the highest rate of production and mass fraction (Fig. 4a). Therefore this specie was used in Fig. 3 for mass fraction analysis. The KHP increases rapidly and decomposes soon after attaining its decomposition temperature. After decomposition, the KHP produces two OH radicals (as indicated by the small rise in temperature and OH concentration on Fig. 3) and this is the branching reaction that gives rise to the low temperature heat release. This is a marker of the first stage ignition, sometimes referred to as cool flame [24]. As the temperature of the mixture increases, equilibrium shifts and RO_2 dissociation is preferred. This decreases the production of KHP while the fuel continues consuming the radicals produced by the KHP. The heat release also decreases and the overall rate of reaction slows down. This produces what is known as the NTC regime. Even though the heat released here is not sufficient to cause the second stage ignition, the first stage ignition is important in combustion systems because it provides early heat release, such that the mixtures reach the second stage ignition temperatures earlier than would have attained without this low temperature heat release [23].

Immediately after the first stage ignition, H_2O_2 is formed primarily from the reaction of nC_7H_{16} plus HO_2. The concentration of H_2O_2 begins to accumulate (see the NTC region on Fig. 3), until it reaches a maximum at 1000K. Below this temperature, the decomposition of H_2O_2 is much slower than its accumulation [23]. At relatively high temperatures, H_2O_2 dissociation begins. The pool of H_2O_2 disappears rapidly producing two OH radicals, as indicated by a sharp rise in temperature (Fig. 3 and Fig. 4b) corresponding to H_2O_2 decomposition having the highest rate. As noted by Westbrook [23], the increase in these OH radicals consumes all the remaining fuel followed by a rapid rise in temperature and thus resulting in the second stage ignition. Therefore, the H_2O_2 plays a big role in the second stage ignition, wherein its disappearance is a marker of the second stage ignition.

After the first stage ignition, formaldehyde (CH_2O) and CO are formed. As seen in Fig. 3, the shape of the curve of CH_2O decomposition after its formation is similar to that of fuel decomposition. Therefore, since formaldehyde is easily accessed by the CH_2O-LIF optical diagnostics, this could be used to determine the fate of the fuel. Likewise, complete disappearance of CO marks the end of the second stage ignition [21].

Second stage ignition delay time:

Effects of injection pressure on diesel and biodiesel ignition delays:

Three different injection pressures of 100 MPa, 200 MPa and 300 MPa were used in order to understand the effects of injection pressure on ignition delay. In Fig. 5, the ignition delays at the three different injection pressures were plotted against the time after start of injection.

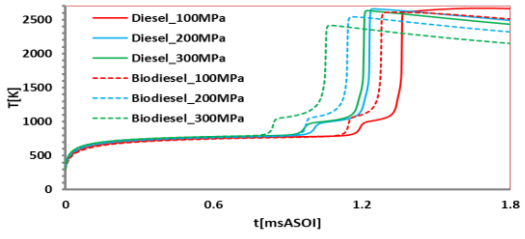

Figure 5 Ignition delay time at 3 injection pressures

The ignition delay is taken as the time after start of injection (ASOI) to the time when the rate of change of

temperature with time is maximum. Increase in injection pressures shortened the ignition delay period for both diesel and biodiesel surrogates. This decrease could be due to increase in mixing that was achieved as the injection pressure is increased [25]. Fig. 5a also shows that the ignition delay of biodiesel surrogate is shorter than that of diesel surrogate at all injection pressures. Similar trends are observed in the experiment. This is because the biodiesel under investigation has a higher CN (64) than diesel (56). CN gives an indication of the ignitability of fuels. Fuels with high cetane number ignite faster. As discussed earlier, the two peaks noted on the plots represent the two-stage ignition delay.

To understand the effect of injection pressure on ignition location, the core temperature was plotted against a non-dimensional axial distance as shown in Fig. 6.

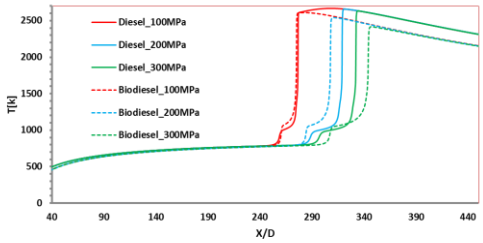

Figure 6 Simulation of effects of injection pressure on ignition location

As injection pressure is increased from 100 to 300 MPa for fuels, the ignition location further shifts downstream. This is attributed to an increase in injection velocity at higher injection pressures [12].

Effect of ambient pressure on ignition delay:

In order to understand the effect of ambient pressure on ignition delay, three different ambient pressures (4, 5 and 6) MPa respectively were considered at different temperatures as shown in Fig. 7. The second stage ignition delay time was plotted against the ambient temperatures.

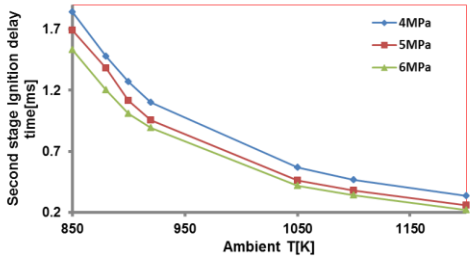

Figure 7. Simulation of ignition delay time at different ambient pressures

The plot shows that at a particular ambient temperature, increase in ambient pressure decreases the ignition delay time. This is in line with the findings of Kobori et al. [13], who reported that ignition delay time is inversely proportional to the ambient gas pressure, suggesting that the ignition of diesel fuel spray is rate controlled by molar concentration of oxygen. At higher ambient pressures, there is an increase in the concentration of oxygen, and this increases the reactivity and shortens the ignition delay time.

Effects of ambient oxygen concentration on ignition delay time:

Reduction in oxygen concentration is mainly useful for the exhaust gas recirculation (EGR) in engines. EGR inhibits the formation of NOx in engines by reducing the flame temperature. However, this is achieved at the expense of increasing emissions of unburned hydrocarbons, and decrease in overall engine cycle efficiency [27]. In order to understand the effects of oxygen concentration on ignition delay time, the core temperature was plotted against time as shown in Fig. 8a. Two different ambient oxygen concentrations; 21% and 12% were considered.

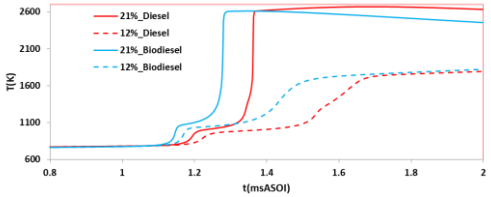

Figure 8 Ignition delay time at 21% and 12% O_2 concentrations

For both fuels, decreasing the oxygen concentration from 21% to 12% increases the ignition delay time. At the lower oxygen concentrations, the rate of reaction decreases, as indicated by lowering of combustion temperature. Also, less heat is released at the end of the first stage ignition leading to an increase in the overall ignition delay time at lower O_2 concentration. As noted on the graphs, the combustion temperature is higher at 21% oxygen concentration, hence reactivity is higher.
Figure 8 shows that the second stage ignition of biodiesel surrogate is lower than diesel surrogate for all the EGR conditions considered.

Conclusion

In this research, the ignition characteristics of diesel and biodiesel fuel surrogates were studied in a constant volume combustion chamber using TSL model. The simulations over predict ignition delay times under all conditions. The model was used to further investigate other properties of diesel and biodiesel ignition.
The results are as follows:
1. The ignition delay time of biodiesel is shorter than that of diesel fuel surrogate at all injection pressures.
2. Increase in injection pressure shortens the ignition delay time for both biodiesel and diesel fuel surrogates. It also shifts the location at which ignition occurs further downstream.
3. Increase in ambient pressure decreases the overall ignition delay time.
4. Decrease in ambient oxygen concentration lengthens the ignition delay time and shifts the ignition location further downstream.

5. Rate of production analysis and mass fraction analysis for diesel fuel surrogate at the end of the first stage ignition showed that NC7KET24 has the highest rate, decomposing to supply early energy to the system. ROP at the end of the second stage ignition showed that the decomposition of H_2O_2 radical into 2 OH gives the much-needed energy that finally ignites the system.

References

1. Herbinet, O., Pitz, W. J., Westbrook, C. K., "Detailed chemical kinetic mechanism for the oxidation of biodiesel fuels blend surrogate," Combust. Flame 2010 DOI:10.1016/J.

2. Luo, Z., Plomer, M. Lu, T.F., Som, S., Longman, D.E., Sarathy, S.M., Pitz, W.J., "A Reduced Mechanism for Biodiesel Surrogates for Compression Ignition Engine Applications," Fuel Vol. 99 pp. 143–153, 2012.

3. Kuti O. A., Nishida K., Sarathy M., Zhu J., "Fuel Spray Combustion of waste Cooking Oil and Palm Oil Biodiesel: Direct Photography and Detailed Chemical Kinetics," SAE Technical Paper 2013-01-2554, 2013.

4. Westbrook, C. K., "Biofuels Combustion," Annu. Rev. Phys. Chem. Vol. 64: 201-219. DOI: 10.1146/annurev-physchem-040412-110009.

5. Kuti O.A., Sarathy, S.M., "Numerical studies of Spray Combustion Processes of Palm Oil Biodiesel and Diesel Fuels using Reduced Chemical Kinetic Mechanisms," SAE Technical Paper

6. Szybist J.P., Song, J., Alam, M., Boehman, A.L., "Biodiesel Combustion, Emissions and Emission Control," Fuel Process. Tech. 88(2007):679-691, 2007, doi:10.1016/J.FUPROC.2006.12.008.

7. Zhang J., Jing, W., Roberts, L.W., Fang, T., "Soot Temperature and KL Factor for Biodiesel and Diesel Spray Combustion in a Constant Volume Combustion Chamber," Applied Energy 107(2013):52-65, 2013, doi: 10.1016/J.APENERGY. 2013.02.023.

8. Zhang, X., Gao, G., Li, L., Wu, Z., et al., "Characteristics of Combustion and Emissions in a D.I. Engine Fueled with Biodiesel Blends from Soybean Oil," SAE Technical Paper 2008-01-1832, 2008, doi:10.4271/2008-01-1832.

9. Kousoulidou, M., Fontaras, G., Ntziachristos, L., Samaras Z., "Evaluation of Biodiesel Blends on the Performance and Emissions of a Common-rail Light-Duty Engine and Vehicle," SAE Technical Paper 2009-01-0692, 2009, doi: 10.4271/2009-01-0692.

10. Veltman, M.K., Karra, P.K., Kong S-C., "Effects of Biodiesel Blends on Emissions in Low Temperature Diesel Combustion," SAE Technical Paper 2009-01-0485, 2009 doi: 10.4271/2009-01-0485.

11. Deepak A, Sinha S, Agarwal KA. Experimental investigation of control of NO_X emissions in biodiesel–fueled compression ignition engine. Renew Energy 2006; 31:2356–69.

12. Alfazazi, A., Kuti, O.A., Sarathy S.M., "Two-Stage Lagrangian Modelling of Diesel Spray Combustion". Int. Symp. On Convective Heat and Mass transfer (2014).

13. Kobori, S., Kamimoto, T., Aradi, A.A., A study of Ignition Delay of Diesel Fuel Sprays, Int. J. of Engine Res., 2000, Vol. 1, No. 1, pp. 29-39.

14. Khanh, C., Meghraj, B., Anqi, Z., Seong, Y.L., Numerical Study on Emission Characteristics of High-pressure Dimethyl Ether (DME) Under Different Engine Ambient Conditions, SAE Technical Paper 2013-01-0319.

15. Lutz, A.E., Broadwell, J.E., Simulation of Chemical kinetics in Turbulent Natural Gas Combustion, Final Report GRI-97/0367, Vol. 298, pp. 2-89.

16. Pickett, L.M., Caton, J.A., Musculus, M.P.B., Lutz, A.E., Evaluation of the Equivalence Ratio-temperature Region of Diesel Soot Precursor Formation Using a two-stage Lagrangian Model, Int. J. Engine Res., 2006, Vol. 7, pp. 349-370.

17. Dongee, H., Mungal, M.G., Production of NOx Control by Basic and Advanced Gas Reburning Using the Two-Stage Lagrangian Model, Combust. Flame, 1999, Vol. 119, pp. 483-493.

18. Lutz, A.E., Broadwell, J.E. [1997], "A Turbulent Jet Chemical Model: NOX Production in Jet Flames," Combust. Flame 1998, 114:319-335.

19. Mehl M., Pitz W.J., Westbrook C.K., Curran H.J., "Kinetic Modeling of Gasoline Surrogate Components and Mixtures under Engine Conditions," P. COMBUST. INST. 201133:193-200.

20. Curran, H. J., Gaffuri, P., Pitz, W. J., Westbrook, C. K., "A Comprehensive Modeling Study of n-Heptane Oxidation" Combust. Flame 1998, 114:149-177.

21. Mark P.B. Musculus, Paul C., Miles, Lyle M. Pickett, "Conceptual models for partially premixed low-temperature diesel combustion," Prog. Energ. Combust. Science 01/2013;246–283.

22. Naik, C. V., Westbrook C. K., Herbinet O., Pitz, W. J., Mehl, M., Detailed chemical kinetic mechanism for biodiesel components methyl stearate and methyl oleate. PROC. COMBUST. INST. 2011, 33, pp.383-389.

23. Westbrook C. K., "Chemical kinetics of hydrocarbon ignition in practical combustion systems," PROC. COMBUST. INST. doi: 10.1016/S0082-0784(00)80554-8.

24. Bogin, G. E. Jr., Osecky, E., Ratcliff, Jon Luecke A., et al., "Ignition Quality Tester (IQT) Investigation of the Negative Temperature Coefficient Region of Alkane Autoignition," Energy & Fuels 2013, 27 (3), pp 1632–1642.

25. Kuti, O.A., Wang, X.G., Zhang, W., Nishida, K., et al., "Effect of Injection Pressure on Ignition, Flame Development and Soot Formation Processes of Biodiesel Fuel Spray," SAE Technical Paper. Doi:2010-32-005320109053.

26. Dongee, H., Mungal, M.G., Production of NOx Control by Basic and Advanced Gas Reburning Using the Two-Stage Lagrangian Model, Combust. Flame, 1999, Vol. 119, pp. 483-493

27. Pickett, L.M., "Low flame temperature limits for mixing-controlled Diesel combustion," PROC. COMBUST. INST. doi:10.1016/J. 2013.06.009